

Tunability of silicon carbide resonators with electrothermal actuation and piezoelectric readout.

E. Mastropaolo^a, B. Sviličić^{a,b} and R. Cheung^a

^a*Institute for Integrated Micro and Nano Systems, University of Edinburgh, West Mains Road, Edinburgh EH9 3JF, UK*

^b*University of Rijeka, Studentska ulica 2, 51000 Rijeka, Croatia*

Microelectromechanical systems (MEMS) resonators are being investigated intensively for replacing filter components¹ and quartz crystal² for real time clock application in electronic devices. Silicon carbide (SiC) is an optimal material for implementing robust and reliable MEMS resonant structures as it possesses excellent mechanical and thermal properties³. In our work, we develop SiC resonant structures actuated electrothermally and sensed piezoelectrically⁴. Electrothermal transduction offers major advantages such as simple fabrication process, low actuation voltages, straightforward impedance matching and efficient tuning⁵. Piezoelectric transduction offers stronger electromechanical coupling, easier impedance matching and relatively simpler fabrication process compared to electrostatic transduction⁶. One of the main challenges for MEMS resonators arise from temperature-dependent frequency shifts that obstacle large scale commercialization of MEMS oscillators⁷. Therefore, the tunability of MEMS resonators is of key importance for compensating drifts in frequency due to fabrication process and environmental factors (temperature, humidity and pressure). In order to address frequency drift issues and the possibility of achieving large tuning ranges, we use electrothermal excitation for controlling the devices' operating frequency with an approach similar to Temperature-Controlled Crystal Oscillators.

In this paper, input (electrothermal) driving ports and output (piezoelectric) readout ports have been integrated on top of double-clamped 3C-SiC beams. The devices have been fabricated with beam lengths of 150 μm and 200 μm and widths from 50 μm to 90 μm . Fig. 1 shows side and top view schematics of the designed devices. Fig. 2 shows a scanning electron micrograph of one of the fabricated structures together with one of the transmission magnitude plots obtained with the measurements. Resonant frequencies in the range 0.9 MHz – 1.9 MHz have been measured. The devices' frequency can be tuned to $\sim 300,000$ ppm and Q-factor can be improved by $\sim 130\%$ using relatively low d.c. input bias voltage (1 V – 7 V). The influence of beam dimensions on shifts of resonant frequency and Q-factor during tuning has been investigated. As the beam width increases the tuning range decreases (Fig. 3) and Q-factor decreases (Fig. 4). Furthermore, the design length of input port (L_{in} in Fig. 1b) has been investigated for maximizing both tunability and Q-factor. Details on devices' design, materials, fabrication process and testing procedure will be presented. The measurements results obtained by testing the fabricated devices will be discussed along with the influence of the structures' dimension on frequency shift, Q-factor and energy dissipation.

Acknowledgment: B. Sviličić acknowledges financial support of the Croatian Science Foundation.

¹ C.S. Lam, Int. Ultrason. Symp. Proc. 694, 2008.

² C. T.-C. Nguyen, IEEE Trans. Ultrason. Ferroelectr. Freq. Control, **54**, 251, 2007.

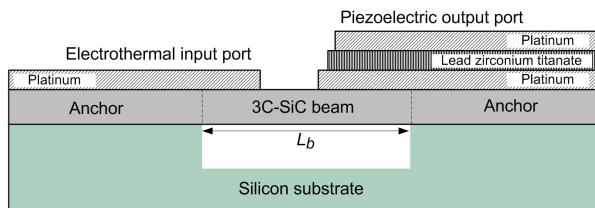
³ R. Cheung, *Silicon carbide micro electromechanical systems*, Imperial College Press, 2006.

⁴ B. Sviličić *et al.*, IEEE Electron Dev. Lett., **33**, 278, 2012.

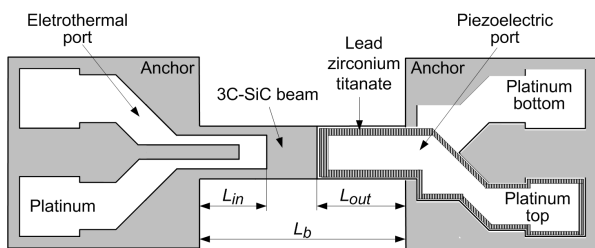
⁵ T. Remtéma *et al.*, Sens. and Act. A, **91**, 326, 2001.

⁶ D. L. DeVoe, Sens. and Act. A, **88**, 263, 2001.

⁷ B. Kim *et al.*, IEEE Int. Freq. Control Symp., 1, 2010.

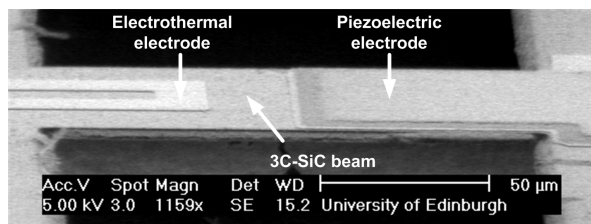


a)

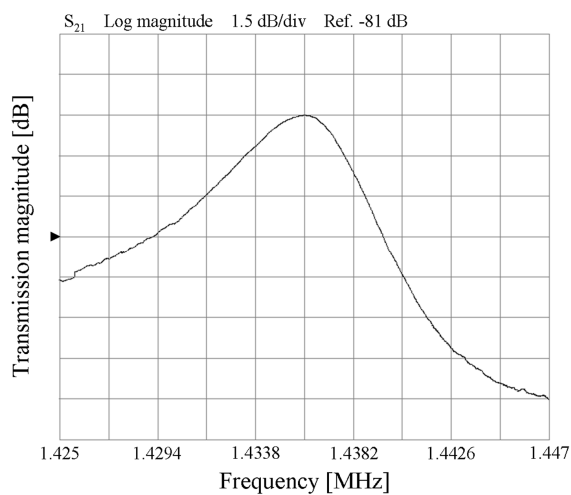


b)

Figure 1: Schematic of the designed device with the beam length L_b and electrodes lengths relation.



a)



b)

Figure 2: (a) Scanning electron micrograph of one of the fabricated structures. (b) One of the measured transmission magnitude frequency response.

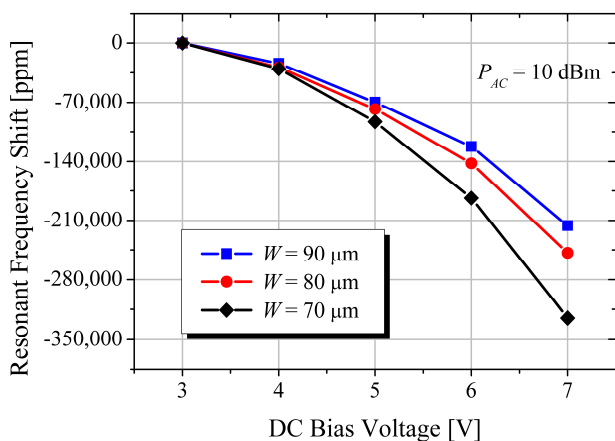


Figure 3: Measured resonant frequency shift as a function of DC bias input voltage for different beam widths W .

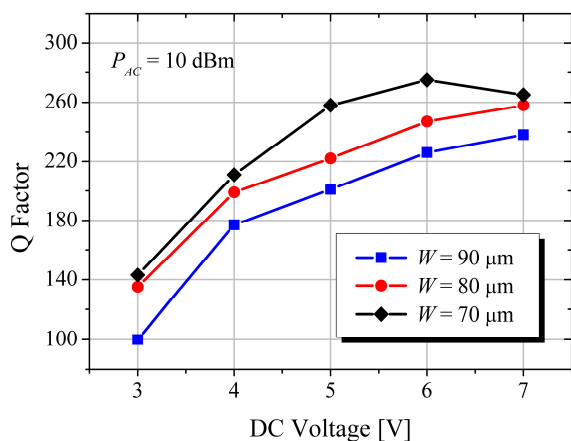


Figure 4: Measured Q-factor in air as a function of DC bias input voltage for different beam widths W .